CHALMERS

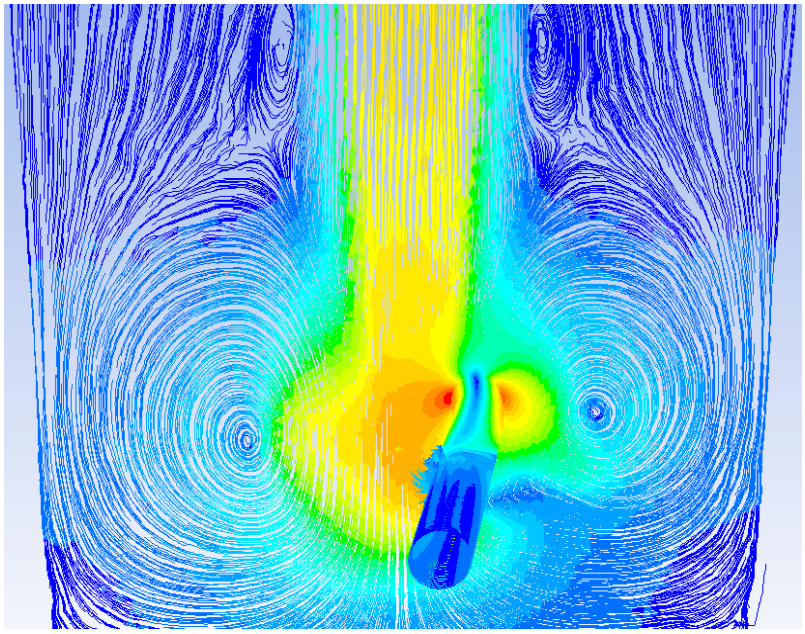

Mattias Wångblad

*** Pressure studies in water jet simulations**

Department of Applied Mechanics
Division of Fluid Dynamics
Chalmers University of Technology
Göteborg Sweden, 2011

Master's Thesis [2011 : 53]

Master's Thesis 2011:53

Pressure studies in water jet simulations

Master's Thesis

Mattias Wångblad

Department of Applied Mechanics
Division of Fluid Dynamics
Chalmers University of Technology
Göteborg, Sweden, 2011

Pressure studies in water jet simulations
Master's Thesis
Mattias Wångblad

Master's Thesis 2011:53

Department of Applied Mechanics,
Division of Fluid Dynamics
Chalmers University of Technology
Se-412 96 Göteborg, Sweden
Phone +46-(0)31-7721400
Fax: +46-(0)31-180976

Printed at Chalmers Reproservice
Göteborg, Sweden 2011

Pressure studies in water jet simulations

Master's Thesis

by

Mattias Wångblad

wangblam@student.chalmers.se

Department of Applied Mechanics

Division of Fluid Dynamics

Chalmers University of Technology

Abstract

This thesis studies the forces on a coolant pipe in wetwell from waterjets after a full scale loss-of-coolant-accident(LOCA) in a nuclear reactor. The waterjets are part of a pressure suppression system constructed to be able to take care of ruptures in the reactor.

Thermodynamical simulations in RELAP5 show that, at the bottom of drywell, there is an initial pressure wave in drywell during the first 20ms. After this the pressure rises almost linearly during the first second to 324 kPa gauge pressure.

Fluid flow simulations in FLUENT show that the water initially standing in the blowdown pipes is blown out 570ms after the LOCA with a final speed of 14 m/s. As the coolant pipe is hit by the jet it experiences oscillating forces with a maximum of 13 kN/m after 900ms. The simulations were performed using the $k - \epsilon$ model. These forces are satisfactory low for the pipe not to break during a LOCA.

Keywords:LOCA,nuclear safety,Pressure suppression, RELAP5, FLUENT, Jet impingement

Acknowledgement

I would like to thank FS Dynamics for making it possible to perform this master thesis.

I would especially like to thank Magnus Ohlson, Mikael Stallgård and Fredrik Carlson for their help, support and interesting discussions during the spring and summer.

Finally a also would like to thank my examiner professor Lars Davidson for his help during the thesis.

Nomenclature

α	Volume fraction of gas or fluid
ϵ	Turbulent dissipation rate
Γ	Transition rate between phases
κ	Wavenumber of eddie movement
μ	Viscosity
ν	Kinematic viscosity
ρ	Density
σ	Turbulent model constant
τ	Timescale
A	Area
B	Body force
$C_1\epsilon$	Turbulent model constant
C_{trans}	Heat transfer coefficient
$DISS$	Dissipation term
FIG	Friction force coeffiecient between two phases
FWG	Wall friction drag coefficient
h	Entalphy
k	Turbulent kinematic energy
L	Length

p	Pressure
Q	Heat energy
q	Heat flux
S	Mean strain rate
T	Temperature
t	Time
U	Internal energy
v	Velocity
W	Work performed by the system

Contents

Abstract **v**

Acknowledgement **vi**

Nomenclature **vii**

1 Introduction **1**

2 Pressure suppression system **3**
2.1 Studied geometry 5

3 Thermodynamical simulations in RELAP5 **7**
3.1 Mass conservation 7
3.2 Momentum conversation 8
3.3 Energy conservation 8
3.3.1 Wall heat transfer 9
3.3.2 Interface heat transfer 9
3.3.3 Dissipation terms 11
3.4 Solution 11

4 Impinging jets **13**
4.1 Equations governing motions of fluids 13
4.2 Turbulence 14
4.3 Energy cascade 14
4.4 Length and timescales 15
4.5 Turbulence models 16
4.5.1 Reynolds averaged Navier Stoke (RANS) 17
4.5.2 Unsteady RANS 18
4.5.3 Large Eddy simulation (LES) 20

5 Simulation methods **21**
5.1 Simulations in RELAP5 21
5.2 Simulations in FLUENT 22
5.2.1 Mesh 22
5.2.2 Computations 23
5.2.3 Choice of turbulence model 24
5.3 Pipestress 25

6 Results and discussion **27**
6.1 Pressure build up 27
6.2 Blown out jet 28
6.3 Forces on the pipe 29
6.4 Jet profile around the pipe 33
6.5 Choice of model 35
6.6 Timescales 36
6.7 Effects on the pipe 36
6.8 Conclusions 36

Appendix A: RELAP5 input file **40**

Appendix B: Force calculation UDF **44**

Chapter 1

Introduction

Nuclear power plants have high demands on safety and every part within them are evaluated and tested. This thesis focuses on studying the effects of water jets hitting coolant pipes in a water pool. The jets are part of an emergency depressurising system in the case of a rupture on one of the main circulation pipes in the reactor. The rapid expansion of hot pressurised water/steam leads to an increased pressure in an open airspace. This increased pressure will push down water standing in 96 blowdown pipes into a water pool thus creating water jets.

Previous studies have been deemed unsatisfactory by the Swedish nuclear power industry so this thesis aims at studying the full course of events more rigorously. The thesis follows the whole course of events from the breakage, with the thermodynamical pressuring, to fluid simulations of the movements of the jets.

The work and simulations have been performed at FS Dynamics in Göteborg with the help of senior consultants in CFD and thermodynamics. The computations were performed in three programs; RELAP5, FLUENT and PipeStress.

Chapter 2

Pressure suppression system

The pressure suppression system (PS) is designed to handle loss-of-coolant-accidents (LOCA). It also serves as containment for radioactive materials leaking in case of an accident and is designed to handle a full scale core melt-down. It was originally designed for boiling water reactors (BWR) but it has also been employed in pressure water reactors (PWR). The system can also be used as a safety pressure relief system if the pressure increases too much in the reactor [1].

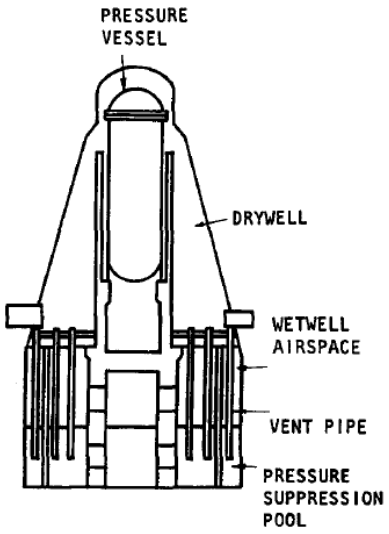

Figure 2.1: *A schematic view of the a Mark II pressure suppression system. Taken from [9].*

The system consists of two main sections. One air filled volume called "the drywell" surrounding the reactor and one water pool called "the wetwell"

located beneath the the drywell. The wetwell consists of a water pool and a large air filled volume. The two volumes are connected through a number of blowdown vents, leading from the bottom of the drywell down into the wetwell. A sketch of the design can be seen in figure 2.1.

The main feature of the wetwell is to condensate steam from a LOCA and thereby diminish the pressure build up since water takes up less space than steam. In the case of a LOCA, steam initially flows into the drywell, continues down through the blowdown vents and finally ends up in the wetwell where it is condensated.

To take care of radioactive materials a sprinkler system sprays in the drywell binding radioactive gases to water droplets which fall down into the water pool. In the case of a full core, the radioactive material falls into the pool and is thus at least partially cooled. [1]

Modern designs of the PS system blows the jets horizontally into the wetwell with nozzle to prevent jets. But in older systems like the one studied here, the process after a LOCA consists of four stages: [1]

- The pressure build-up in the drywell pushes down the water pile that initially is standing in the blowdown vents, creating jets that are shot down into the wetwell.

- The waterlevel in the wetwell rises from the sudden inflow of steam into the pool until it hits the ceiling and falls back down.

- A phenomena called condensation oscillations (CO) occurs at the outlet of the blowdown vents emerging from collapsing steam bubbles.

- When the flow rate diminisshes the CO:s turn into a slower more violent form of oscillations called chugging.

During the first stage pressure is only built up in the drywell where it rises quickly. This accelerates the water standing in the blowdown pipes sending down a water jet into the pool. This jet only affects components directly or almost directly beneath the pipes but gives rise to a quite large sudden rise in pressure at the bottom of the pool.

When all water has been cleared from the blowdown pipes, steam starts being blown into the pool. The sudden inflow of steam causes the water level to be pushed upwards until it hits the ceiling and falls down again. This affects all components placed above the initial water line.

When steam comes out of the vents it forms a bubble as a surface against the water. In the interface, between the hot steam and the cold water, the steam is condensated and falls into the pool. As the bubbles grow, they

eventually turn unstable and collapse back into the vent and then start to reform. This is what is called condensation oscillations and happen at a rate of around 10Hz. These oscillations send out pressure waves when the bubbles collapse.

As the pressure in the reactor is reduced, the flow rates starts to diminish. At lower flow rates through the blowdown pipes the condensation oscillations turns into another oscillating effect called chugging. This phenomenon is slower and occurs with about 1 Hz, but is instead more violent.

2.1 Studied geometry

This report focuses on the effects from the water jets coming from the blowdown pipes. In the design used here there are 96 blowdowns pipes arranged in 16 radial lines, each with 6 pipes, see figure 2.2. The pipes have a diameter of 600mm, a total length of 14,5 m of which 3m is located underneath the initial waterlevel in the the wetwell. The initial waterlevel in the the wetwell is set to 7m.

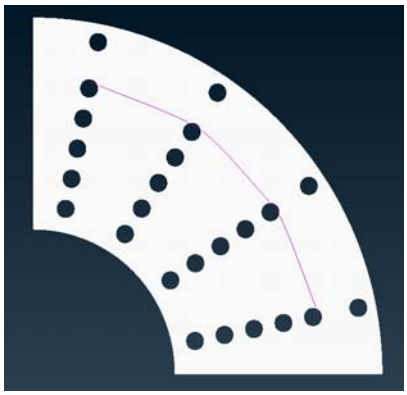

Figure 2.2: *Schematic view over the placements of the blowdown pipes and the coolant pipe underneath some of the blowdown pipes. A quarter of the total area is shown.*

Directly underneath a few these of these vertical blowdown pipes, a system of horisontal pipes is located which are used for cooling the wetwell after an accident. It is the effects of the jets from the vertical pipes on these horisontal pipes that is the aim of this thesis to determine. The horisontal pipes have a diameter of 205mm and those exposed from the waterjets lie horisontally with their center 2,8m underneath the blowdown pipes. The pipes aren't centered exactly under the jets and are therefore not completely cov-

ered by the jets. The effects of their location both vertically and horizontally have been studied in this thesis.

Chapter 3

Thermodynamical simulations in RELAP5

RELAP5 is a one-dimensional thermo-hydrodynamic solver allowing two phase solutions of transport differential equations using a Crank-Nicholson finite difference scheme. The equations emerge from the conversation of mass, momentum and energy for both the gas and liquid phase.

RELAP5 mainly focuses on the thermodynamical equations and heat transfers rather than flow patterns. It operates in only one dimension and it therefore uses highly simplified geometries and does not require complex meshes unlike most FEM programs. The following sections are based on the manual to RELAP5 [14].

3.1 Mass conservation

RELAP5 uses a two-phase model to describe the flow. It is therefore necessary to write equations of conservation for both the gas and the fluid phase. Since at least the steam is highly compressible the change in density can't be neglected as is common when just dealing with incompressible fluids. It is also necessary to take care of the transfer of mass, momentum and energy between the phases at phase transitions, i.e. boiling or condensation.

The equations of conservation of mass can therefore be written as:

$$\frac{\partial \alpha_{\mathrm{g}} \rho_{\mathrm{g}}}{\partial t} + \frac{\partial \alpha_{\mathrm{g}} \rho_{\mathrm{g}} v_{\mathrm{g}}}{\partial x} = \Gamma_{\mathrm{g}} \tag{3.1}$$

$$\frac{\partial \alpha_{\mathrm{f}} \rho_{\mathrm{f}}}{\partial t} + \frac{\partial \alpha_{\mathrm{f}} \rho_{\mathrm{f}} v_{\mathrm{f}}}{\partial x} = \Gamma_{\mathrm{f}} \tag{3.2}$$

where $\Gamma_{\mathrm{f}} = -\Gamma_{\mathrm{g}}$ are transitions between the two phases, $\alpha_{\mathrm{f}} = 1 - \alpha_g$ is the

volume fraction in the fluid phase, v_g and v_f are the velocities, of the gas and fluid respectively, and ρ_g and ρ_f are their densities.

3.2 Momentum conversation

RELAP5 uses a simplified model for momentum conservation. The main purpose of the simulations is to find correct pressures and temperature instead of finding the exact flow patterns. It is therefore acceptable with a slightly less exact formulation of the momentum equation. The convective term is rewritten as:

$$v\frac{\partial v}{\partial x} = \frac{1}{2}\frac{\partial v^2}{\partial x} \tag{3.3}$$

because this form is more convenient for the numerical scheme used by RELAP5. Other simplifications made are that the Reynolds and phasic viscous stresses have been neglected and the phasic pressures are assumed to be equal. The equations for the gas phase can then be written as:

$$\begin{aligned}\alpha_\mathrm{g}\rho_\mathrm{g}\frac{\partial v_g}{\partial t} + \frac{1}{2}\alpha_g\frac{\partial v_g^2}{\partial x} = -\alpha\frac{\partial P}{\partial x} + \alpha_g\rho_g B_x - (\alpha\rho_g v_g)FWG \\ +\Gamma_\mathrm{g}(v_{\mathrm{g}I} - v_\mathrm{g}) - (\alpha_\mathrm{g}\rho_\mathrm{g})FIG(v_\mathrm{g} - v_\mathrm{f}) - C\alpha_\mathrm{g}\alpha_\mathrm{f}\rho_\mathrm{m}\frac{\partial(v_\mathrm{g} - v_\mathrm{f})}{\partial t}\end{aligned} \tag{3.4}$$

with a similar equation for the liquid phase. Here P is the external pressure, B_x is an ordinary body forces e.g. gravity and FWG is the wall friction drag coefficient. The three last terms are internal momentum transfer between the phases and thus conserved within the system. These three terms come from momentum transfer due to phase changes, viscous forces in the interface between the phases and effects from the experienced virtual mass, respectively.

3.3 Energy conservation

Since there is a large difference in specific enthalpy between the two phases, the equations for conserving energy have to deal with vapor generation and condensation. The equations emerge from the first law of thermodynamics:

$$dU = dQ - dW \tag{3.5}$$

where dU is the change in total internal energy, dQ is the flux of energy due to heat transfer and $dW = PdV$ is the work done by the system. Writing

the transport equation for U and writing the time dependent changes of the energies, we get:

$$\frac{\partial \alpha_{\mathrm{g}} \rho_{\mathrm{g}} U_{\mathrm{g}}}{\partial t} + \frac{\partial v_{\mathrm{g}} \alpha_{\mathrm{g}} \rho_g U_g}{\partial x} =$$
$$= -P\frac{\partial \alpha_{\mathrm{g}}}{\partial t} - P\frac{\partial \alpha_g v_g}{\partial x} + Q_{wg} + Q_{ig} - \Gamma_{ig} h_g^* - \Gamma_w h_g^{'} + DISS_g \qquad (3.6)$$

for the gas phase and similar for the liquid phase. Here U_{g} is the specific internal energy for the gas phase, h_g^* and $h_g^{'}$ are the enthalpies associated with phase changes and wall heat transfer respectively. Q_{wg} is the heat transfer rate from the wall to the gas and Q_{ig} is the heat transfer rate at the interface between the two phases. A similar equation can be written for the fluid phase. The following sections explain the meaning of each term.

3.3.1 Wall heat transfer

In RELAP there are two mechanisms for heat transfer, either wall heat transfer or interface heat transfer. The wall heat transfer is the effect of boundary conditions heating up the two phases. The total heat flux q_{tot} from a wall to a two-phase water-steam mixture is calculated as:

$$q_{tot} = C_{trans}(T_w - T) \qquad (3.7)$$

where C_{trans} is the transfer coefficient and T the temperature of the mixture. RELAP5 uses a wide range of models to simulate this heat transfer coefficient C_{trans}, depending on how the temperature T relates to the current saturation temperature at current pressure [15]. The phasic heat flux can then be written as:

$$Q_{wg} = q_{tot} A_{\mathrm{g}} \qquad (3.8)$$

where A_{g} is the area of the gas exposed to the wall and similar for the fluid phase.

3.3.2 Interface heat transfer

RELAP5 uses one temperature for each phase in a volume. The temperatures are calculated on the boundaries and are then used all over the volume. At the interface between the phases, heat exchange is calculated however. This heat transfer comes from differences in the phase temperatures and the saturation temperature, for the current pressure. It is divided into two parts,

interfacial heat transfer between the phases close to a wall Q_i^W and in the main pool (bulk) Q_i^B, so that the total interfacial heat transfer is written as:

$$Q_{ig} = Q_{ig}^B + Q_{ig}^W \tag{3.9}$$

For the bulk this is written as:

$$\begin{aligned} Q_{ig}^B &= H_{ig}(T^s - T_{\mathrm{g}}) && (3.10)\\ Q_{if}^B &= H_{if}(T^s - T_{\mathrm{f}}) && (3.11) \end{aligned}$$

where H_{ig} and H_{if} are the heat transfer coefficients, T^s the saturation temperature and T_{g} the phasic temperature.

At saturation temperature all heat transfer between the phases lead to phase change, i.e. vaporisation or condensation. In RELAP5 it is assumed that this is true for both the interface close to the wall and in the bulk. The equations for transfer of heat between the phases are then written as:

$$\begin{aligned} Q_{ig}^W + Q_{if}^W + \Gamma_w(h_{\mathrm{g}}^{'} - h_{\mathrm{f}}^{'}) &= 0 && (3.12)\\ Q_{ig}^B + Q_{if}^B + \Gamma_{ig}(h_{\mathrm{g}}^{*} - h_{\mathrm{f}}^{*}) &= 0 && (3.13) \end{aligned}$$

As was discussed earlier, RELAP5 uses different models for heat transfer depending on the current temperature relative to the saturation temperature. All phase changes are assumed to happen at saturation temperature and in that regime; all heat flux from the wall is assumed to lead to boiling or condensation dependent on the wall temperature. That is equation 3.12 can then be written, using equation 3.8, as:

$$\Gamma_w = -\frac{q_{tot}A_{\mathrm{f}}}{h_{\mathrm{g}}^{'} - h_{\mathrm{f}}^{'}} \tag{3.14}$$

or

$$\Gamma_w = -\frac{q_{tot}A_{\mathrm{g}}}{h_{\mathrm{g}}^{'} - h_{\mathrm{f}}^{'}} \tag{3.15}$$

depending on if it is a boiling or condensating process respectively.

Finally we can write the phase change due to heat exchange in the interface in the bulk using equations 3.10, 3.11 and 3.13:

$$\Gamma_{ig} = -\frac{H_{ig}(T^s - T_{\mathrm{g}}) + H_{if}(T^s - T_{\mathrm{f}})}{h_{\mathrm{g}}^{*} - h_{\mathrm{f}}^{*}} \tag{3.16}$$

3.3.3 Dissipation terms

The dissipation terms comes from energy losses due to friction in pumps and against walls. They are modelled as.

$$DISS_{\mathrm{g}} = \alpha_{\mathrm{g}}\rho_{\mathrm{g}}FWGv_{\mathrm{g}}^2 \tag{3.17}$$
$$DISS_{\mathrm{f}} = \alpha_{\mathrm{f}}\rho_{\mathrm{f}}FWFv_{\mathrm{f}}^2 \tag{3.18}$$

where FWG and FWF are the forward drag coefficients found in physics tables for different materials.

3.4 Solution

These three conservation equations (mass, momentum and energy) are solved for the two phases in the model every timestep. Solving these yields the volume fractions and temperature for both phases. From this RELAP5 uses thermodynamical tables to calculate the pressure.

Chapter 4

Impinging jets

Impingement is the phenomena of a jet perpendicularly hitting a boundary with high velocity and the deflection of the jet afterwards. This is of great interest for thermodynamical applications since turbulence close to the wall gives increased mixing and thus greater thermal conduction which make impinging jets great coolants. For a jet that hits a pipe, the momentum transfer is also of importance, which is what is studied in this report.

Most studies of impinging jets investigate the impingement against a flat plate. This report study the impingement against a convex surface, i.e. a cylinder, which is not placed directly underneath the jet.

4.1 Equations governing motions of fluids

The main equations when it comes to fluid dynamics are the Navier-Stokes equations [16]:

$$\frac{\partial \rho}{\partial t} + \nabla \cdot (\rho \mathbf{v}) = 0 \tag{4.1}$$

$$\rho \left(\frac{\partial \mathbf{v}}{\partial t} + \mathbf{v} \nabla \cdot \mathbf{v} \right) = \nabla \mathbf{p} + \mu \nabla^2 \mathbf{v} - \mathbf{f} \tag{4.2}$$

They are derived from the equations of conservation of equations of motion and momentum of the fluid and for most boundary conditions these equations can't be solved analytically but have to be solved numerically. A common assumption when dealing with these equations is that the fluid is incompressible i.e. $\frac{\partial \rho}{\partial t} = 0$ and also that the viscosity remains constant throughout the computational domain. This simplifies the first equation (the continuity equation) to:

$$\nabla \cdot \mathbf{v} = 0 \tag{4.3}$$

4.2 Turbulence

A fluid flow can be classified into two different types, laminar or turbulent. In a laminar flow the fluid flows in an ordered fashion with one clear velocity gradient and no local fluctuations, while in a turbulent flow fluid motion is more chaotic, with large fluctuations and whirls emerging. To classify if a flow is laminar or turbulent one normally uses the Reynolds number $Re = \frac{vL}{\nu}$, where L is the relevant length scale e.g. the diameter in a pipe flow and with a high Reynolds number meaning a more turbulent flow.

It is common to talk about eddies when discussing fluid dynamics. Eddies are basically swirls and rotations in a fluid breaking the symmetry of a laminar flow. Eddies are of importance since it is here the turbulence is expressed. The distribution of the number of eddies and their sizes are descriptive for the turbulence and at which length and timescales that are important for the dynamics. Figure 4.1 sketches the eddies and the distribution of kinetic energy stored in them in a turbulent flow.

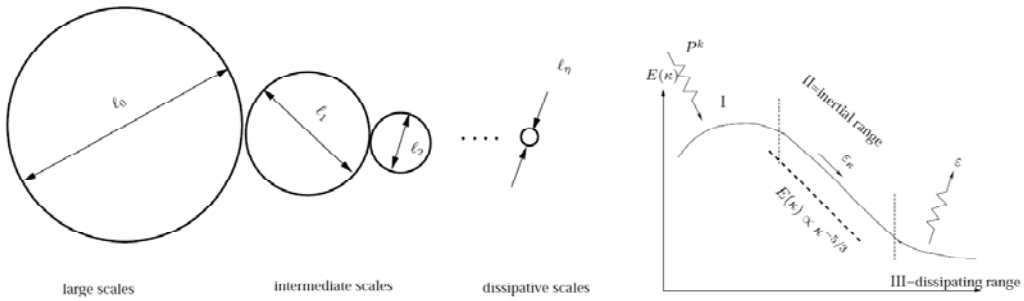

Figure 4.1: *Descriptive picture of eddies, their sizes and correspondence to the total energy stored in them. Turbulent kinetic energy is produced as large eddies and and is transferred to smaller eddies until it is destroyed in the dissipative range. Taken from [6].*

4.3 Energy cascade

Turbulence is created from the shear stresses in the mean flow and first formed as large eddies with high velocities and large circulation lengths. These large eddies interact and give rise to secondary smaller eddies which, in their turn, creates even smaller eddies, and so on by processes called vortex stretching and tilting [6]. Turbulent energy is thus created at the largest eddies and then transferred down to smaller and smaller eddies. At the

smallest eddies noneleastic molecular bumps are dominant which dissipates the energy into heat. This sequence of energy transfer is called the energy cascade. It can be summarised in a short verse by L.F Richardson [2]:

Big whirls have little whirls
Which feed on their velocity
And little whirls have lesser whirls
And so on to viscosity
in the molecular sense

It is more convenient to describe the eddies in terms of wavenumbers instead of size $\kappa = \frac{1}{L}$. Figure 4.1 shows an ordinary distribution of energy versus the wavenumber and also at what scale the Kolomogorov and integral scale act.

Even though some energy is transferred from small scales to larger (called backscattering) this is of minor importance and often omitted in models. Some energy is also lost to heat at larger scales but studies show that 90% is lost at the smallest scale [17].

4.4 Length and timescales

As already seen, the choice of length and timescale for the simulation is of great importance for the stability and accuracy. It is common to talk about two different time and length scale of the turbulence namely the integral and Kologorov-scale. The integral scale is the largest of these and is the length at which the largest eddies gain their energy from the mean flow. [2][13]. It is in the largest eddies that most of the turbulent energy k is stored so it is natural to define a integral velocity $v_0 = \left(\frac{2k}{3}\right)^{1/2}$ that scales with k (each direction gives a contribution to the energy $k_i = \frac{v_i^2}{2}$). The dissipation rate ϵ is defined as the rate at which kinetic energy k is destroyed so it is therefore natural to define a integral timescale $\tau_0 = \frac{k}{\epsilon}$ that is the characteristic time for the turbulent kinetic energy to be dissipated. This gives us the integral lengthscale:

$$l_0 = v_0 \cdot \tau_0 = \frac{k^{3/2}}{\epsilon} \tag{4.4}$$

At the smallest length scale little remains of the quasi-structured large eddies and movements are almost completely random. In 1941 Kolmogorov assumed that at these scales the chaotic behaviour of the particles is isotropic i.e. there isn't a preferred direction for the fluctuations statistically. He also assumed that this behaviour is homogeneous and identical for every turbulent

flow at sufficiently small scales and that it can be described by only ϵ and ν. A dimensional analysis gives:

$$\eta = \left(\frac{\nu^3}{\epsilon}\right)^{1/4} \quad \tau_\eta = \left(\frac{\nu}{\epsilon}\right)^{1/4} \quad u_\eta = (\nu\epsilon)^{1/4} \tag{4.5}$$

where η is the Kolmogorov length scale. The Reynolds number at Kolmogorov scale becomes unity:

$$Re_\eta = \frac{\eta u_\eta}{\nu} = 1 \tag{4.6}$$

The two lengthscales, l_0 and ν, are important when constructing the mesh and deciding time step size. In a LES simulation it is crucial that all the cutoff filter length is small enough to resolve most of the eddies while not computing all the eddies down to the Kolmogorov scale since this is too costly. For a RANS it is important that the timestep length is of the correct order so that eddies are not missed due to averaging over a too long time. [13]. [16]

4.5 Turbulence models

The transition to turbulence is a complex dynamic process which is yet to be fully understood. Since turbulent flow shows highly chaotic behaviour it is greatly dependent of boundary conditions and the computational grid. To fully resolve a turbulent flow it is necessary to have a very fine mesh to account for all small motions. This is called a Direct Numerical Simulation(DNS) and is the most accurate way of modeling a fluid flow but with the huge drawback with the need for a very fine computational grid. This makes the computations very costly in terms of computational time.

A solution for this is to create models that computes the amount of turbulence rather than all the actual motions. These models focuses on computing the amount of turbulence, its transportation and then model how this affects the flow. Different models use different quantities to measure the amount of turbulence. One of the simplest models; Spalart-Allmaras, defines a turbulent viscosity as a measure and solves one additional equation for computing this. The $k - \epsilon$ model requires two extra equations using the kinetic energy of all turbulent fluctuations and the dissipation of this, as a measure of the turbulent length scale. More complex models like the Reynold Stress Model (RSM) needs an additional six equations to compute all shear stresses emerging from turbulent movements.

4.5.1 Reynolds averaged Navier Stoke (RANS)

Since it is often too computational demanding to fully resolve the Navier-Stokes equations (4.1-4.2) it is common to construct a new set of equations that average the eddies movements in time. These are called the Reynolds-Averaged Navier Stokes (RANS) equations from the fact that all quantities are written in the Reynolds decomposition.

$$\mathbf{v} = \bar{\mathbf{v}} + \mathbf{v}' \tag{4.7}$$
$$\mathbf{p} = \bar{\mathbf{p}} + \mathbf{p}' \tag{4.8}$$

where the instantaneous quantity $\mathbf{v}$ has been decomposed into a mean part, $\bar{\mathbf{v}}$ and a fluctuating part $\mathbf{v}'$. Writing the Navier-Stokes equations in this form and time-averaging gives:

$$\overline{\nabla\left(\bar{\mathbf{v}} + \mathbf{v}'\right)} = 0 \tag{4.9}$$
$$\overline{\frac{\partial(\bar{\mathbf{v}} + \mathbf{v}')}{\partial t}} + \overline{(\bar{\mathbf{v}} + \mathbf{v}')\nabla(\bar{\mathbf{v}} + \mathbf{v}')} = \tag{4.10}$$
$$= \overline{\mathbf{f} + \mathbf{f}'} - \frac{1}{\rho}(\overline{\bar{\mathbf{p}} + \mathbf{p}'}) + \nu\overline{\nabla^2(\bar{\mathbf{v}} + \mathbf{v}')}$$

Per definition the mean of the fluctuating part is zero i.e. $\overline{\mathbf{v}'} = 0$ and the the time average of an already averaged quantity remains constant $\overline{\bar{\mathbf{v}}} = \bar{\mathbf{v}}$. The two equations are then reduced to:

$$\rho(\frac{\partial v_i}{\partial t} + \rho\bar{v_j}\frac{\partial v_i}{\partial x_j}) = \rho f_i + \frac{\partial}{\partial x_j}\left[-\bar{p}\delta_{ij} + \mu S_{ij} - \rho\overline{v_i' v_j'}\right] \tag{4.11}$$

When written in Einstein notation, where $S_{ij} = \frac{1}{2}\left(\frac{\partial \bar{u_i}}{\partial x_j} + \frac{\partial \bar{u_j}}{\partial x_i}\right)$ is the mean shear stress tensor. The last terms $\rho\overline{v_i' v_j'}$ are called the Reynolds stresses which are the turbulent stresses emerging from turbulent fluctuations. Since this Reynolds stress tensor is symmetrical, there are six different Reynolds stresses. These new stresses have to be solved in order to resolve the new RANS equations and this is called the closure problem.

There are a number of models used to solve the closure problem. One is the Reynolds Stress Model (RSM) where new transport equations are constructed for each of the six stresses and then solved in the same way as for the transport of momentum and mass. This is quite costly since it increases the number of equations from 4 to 10 which has to be solved each iteration. Instead there exist several simpler models with fewer equations using

Boussinesq assumption:

$$\overline{\rho u_i' u_j'} = -2\nu_t S_{ij} + \frac{2}{3}\delta_{ij}k \tag{4.12}$$

where k is the turbulent kinetic energy computed by taking the trace of the Reynolds stress tensor i.e. $k = \frac{\overline{u_i u_i}}{2}$ and ν_t is the turbulent kinetic viscosity.

The modeling of this turbulent viscosity differs between different turbulence models.

4.5.2 Unsteady RANS

Since all RANS-models use time-averaging when computing the flow it is clear that they are supposed to compute steady state solutions. To find a transient unsteady solution it is therefore necessary to resolve for a timescale a lot larger than that of which is used in the time-averaging. Simulations of this type are called Unsteady RANS or URANS.

$K-\epsilon$ model

One of the most widespread and used models within industrial CFD is the $k-\epsilon$ model. It is based upon transport of the turbulent kinetic energy k and the dissipation rate ϵ which is the rate at which turbulent kinetic energy is transformed into heat by friction. Both quantities follow transportation equations which can be derived from the transportation of the viscous stresses, see for example [6]. The k-equation looks like:

$$\frac{\partial k}{\partial t} + \mathbf{v}\cdot\nabla k = \nabla\cdot[(\nu + \frac{\nu_t}{\sigma_k})\nabla k] + \nu_t S^2 - \epsilon \tag{4.13}$$

The first term on the right side is the ordinary diffusion of k, the second is the production of k from the mean flow through turbulent stresses and finally the third term is the destruction of k which per definition is ϵ. S is the mean strain rate $S = \sqrt{2S_{ij}S_{ij}}$. The equation for ϵ is very similar and looks like:

$$\frac{\partial \epsilon}{\partial t} + \mathbf{v}\cdot\nabla \epsilon = \nabla\cdot[(\nu + \frac{\nu_t}{\sigma_\epsilon})\nabla \epsilon] + C_{1\epsilon}\frac{\epsilon}{k}S^2 - C_{2\epsilon}\frac{\epsilon^2}{k} \tag{4.14}$$

The turbulent viscosity is modeled by:

$$\nu_t = C_\mu \frac{k^2}{\epsilon} \tag{4.15}$$

Table 4.1: *The standard values of the constants for the $k-\epsilon$ model*

C_μ	$C_{1\epsilon}$	$C_{2\epsilon}$	σ_k	σ_ϵ
0.09	1.44	1.92	1	1.3

$C_\mu, C_{1\epsilon}, C_{2\epsilon}, \sigma_k$ and σ_ϵ are model constants tuned to experimental data for best performance. Their standard values which was also used in the simulations can be seen in table 4.1.

The $k-\epsilon$ model is the most used model because of its relative simplicity while still having decent accuracy. It only adds two equations to wrap up the closure problem and has good numerical stabilty.

One problem with the $k-\epsilon$ model is the accuracy close to walls. Close to a wall the friction of the wall slows down the fluid causing increased shear stresses and increased viscous forces in the area. It is common to use a no-slip condition on the wall meaning that the velocity is zero just next to the wall. This is troublesome, especially if the mesh is course and if the fluid has high velocity. This is solved by using a wall function which smoothes the gradient close to the wall.

$k-\epsilon$ realisable

A modification to the model is the the realisable $k-\epsilon$ model which prevents the stresses from becoming negative. Instead of a constant value of C_μ this is instead seen as a variable depending on the local turbulence, vorticity and strain rates. The transport equation for ϵ is changed to:

$$\frac{\partial \epsilon}{\partial t} + \mathbf{v}\cdot\nabla\epsilon = \nabla\cdot[(\nu + \frac{\nu_t}{\sigma_\epsilon})\nabla\epsilon] + C_1 S\epsilon + C_{1\epsilon}\frac{\epsilon}{k}\nu_t S^2 - C_2\frac{\epsilon^2}{k+\sqrt{\nu\epsilon}} \quad (4.16)$$

The new model constant C_1 is defined as $C_1 = max[0.43, \frac{\eta}{\eta+5}$, where $\eta = S\frac{k}{\epsilon}$. The viscosity coefficient C_μ is changed to the form $C_\mu = \frac{1}{A_0 + A_s\frac{kU^*}{\epsilon}}$ where the A_0 is a new model constant and A_s and U^* are coefficients depending on the local rotational velocities and strains.

This realisable version of the $k-\epsilon$ has been found to perform better than the standard version because of the adaptation of its coefficients.

V2f-model

The v2f model also uses k and ϵ with the additional variables v'^2 and f. The idea behind it is to model the wall normal stresses better without the

use of wall models. Therefore it calculates and transports the wall normal fluctuations $v^{'2}$ and a relaxation function of its production f. The turbulent viscosity is then calculated as $\mu = C_\mu v^{'2} \frac{k}{\epsilon}$. This gives a better representation of the turbulence production close to walls and performs much better for impinging jets than the standard $k - \epsilon$ model.

4.5.3 Large Eddy simulation (LES)

The Large Eddy Simulation, commonly just referred to as LES, is unlike the RANS models a completely transient model. Where a RANS model filters in time the LES model employs a spatial filtering instead. The idea is that all eddies larger than a certain characteristic cut-off size will be fully resolved. For turbulent eddies smaller than the cut-off filter length a (often simple) model is used. For large eddies this means very good accuracy while it still it is a lot cheaper than a DNS.

Chapter 5

Simulation methods

The simulations were performed in two stages. First, a simulation of the pressure built up in the blowdown pipes was performed using RELAP5. This pressure was then used as an external boundary condition in a CFD simulation of the water jet, using FLUENT. Studies have been made for interaction between these two codes but since this model has an one way process, with no effect from wetwell to drywell, this wasn't necessary for this thesis.

5.1 Simulations in RELAP5

The model used in the RELAP simulations consist of three parts: the reactor, drywell and an initialisation volume. The initial conditions for drywell and reactor tank can be seen in table 5.1.

Table 5.1: *Initial conditions of the reactor and drywell.*

-	Drywell	Reactor
Temperature	40°C	286°C
Pressure	0,955 bar	70 bar
Volume	5463 m^3	-
Relative humidity	20 %	100 %
Initial breakage flow	-	23 400 kg/s

The scenario modeled was a worst case scenario which is a rupture of one of the main circulation pipes giving a great initial flow of pressurised water. The reactor was modeled as an infinite source with constant pressure and temperature. This was assumed since the initial amount of water and

steam in the reactor is 236 000 kg and the duration of the analysis is less than 2 seconds. It is conservative to assume a constant pressure in favor of decreasing pressure. The flow at the breakage is ramped up linearly during 10ms which is the commonly accepted time for a complete rupture of a pipe in Sweden[10].

The drywell was modeled as a chopped off cone with a connection to the reactor at the top. It was divided into 50 sections with equal height but varying area, connected vertically to each other. This was done because RELAP5 uses a constant temperature and pressure for each phase in a volume. The pressure was measured at the bottom of drywell and it was assumed to be lossless when entering the blowdown pipes.

The initalisation volume was created to give a correct initial humidity in drywell and was modeled with an infinite source. It was connected to drywell with a valve that was closed before the breakage.

The input file for the simulations can be seen in appendix A.

5.2 Simulations in FLUENT

The computational domain was restricted to a volume around one of the blowdown pipes. Only the water filled part of wetwell was modelled, since it is only the jet that is of interest. Since it is an axisymmetric jet and the pipe is symmetric in one direction, the volume was divided in half with a symmetry plane. The domain can be seen in figure 5.1.

The walls at the bottom, the blowdown pipe and the coolant pipe was modelled with a no slip condition. Two walls also have symmetry conditions since similar blowdown pipes exists at both theses sides. The last side, which is opposite of the green side in figure 5.1, and the top of the domain were pressure outlets. The top of the blowdown pipe was an inlet with the, from RELAP5, calculated pressure as boundary condition.

5.2.1 Mesh

The mesh was created in ANSA and was divided into three seperate parts. One was in the inlet pipe, one surrounding the coolant pipe and one for the remaining volume. The mesh can be seen in figures 5.2 - 5.3. There were a total number of 2.9 million elements. The area around the coolant pipe was a pure hex mesh with the closest element at a distance of 0.35mm from the pipe and with a volume growth rate of 1.2 further from the pipe. The domain underneath the blowdown pipe was mainly hex mesh with a side

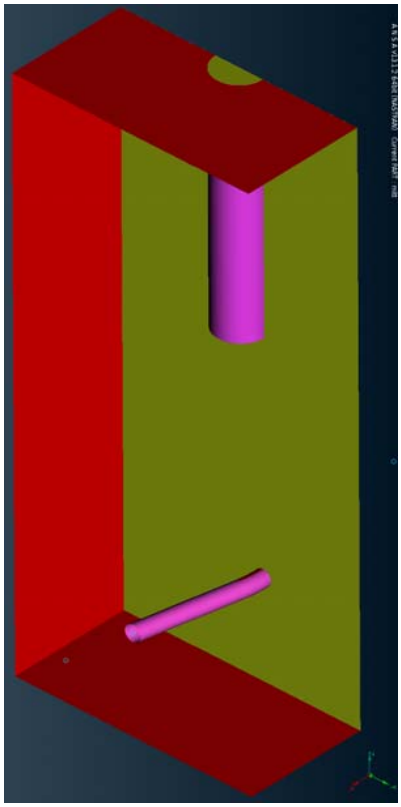

Figure 5.1: *The computational domain. The x-axis is along the coolant pipe in the bottom. The y-axis is to the right in the figure and the z-axis is vertical along the blowdown pipe.*

length of 15mm just beneath the pipe and growing further away. The inlet was meshed with tetrahedral elements with a side length of 30mm.

5.2.2 Computations

Transient simulations were performed with a timestep length of 1ms to have keep a courant number below 20. For the pressure velocity coupling the PISO algorithm was used and PRESTO! was used as pressure discretisation since this is more accurate than the standard method for high Reynolds numbers [12].

A two-phase solution was undesirable and would cause convergence problems and a large increase in computational time. Therefore a single phase model was used, with water continuously being entered into the inlet. By integrating the volume of water, passing from the blowdown pipe into the main domain, it was possible to calculate when the original pile of water

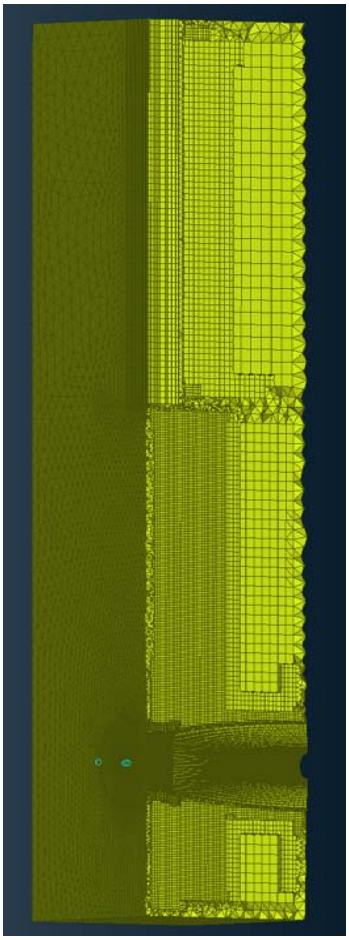

Figure 5.2: *The whole mesh cut in the middle of the y-axis. It contains a total of 3 million elements The folw enters in the middle at the top boundary.*

would have been shot out. When this happened the pressure was lowered slightly and held constant throughout the rest of the simulation.

An User Defined Function (UDF) was used to calculated the force from the static pressure on the coolant pipe at 5 different sections of it at every timestep. The drag from frictional shear stresses on the pipe was omitted since these were measured to be too small to have any real effect. The code can be seen in appendix B.

5.2.3 Choice of turbulence model

The $k - \epsilon$, v2f and LES models were tested.

Due to the large geometry and high velocities it was however not possible

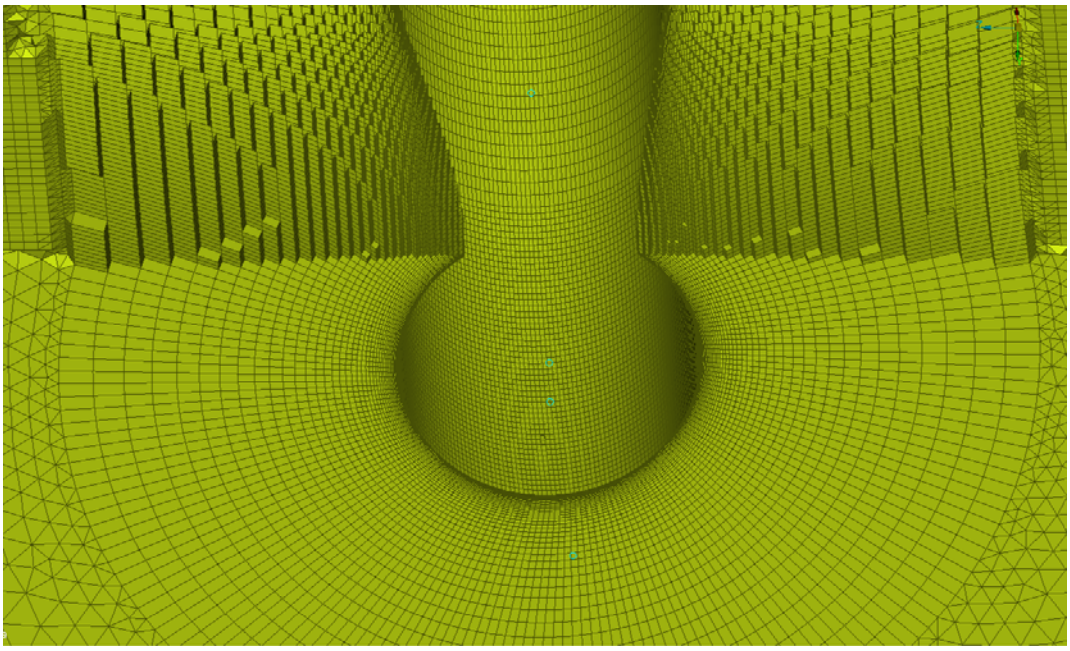

Figure 5.3: *Enlarged view of the mesh of the coolant pipe.*

to create a satisfactorily fine mesh to have a correct LES model, which should have a sidelength in the size of 1/60:th integral scale, i.e. around 1mm, (see section 4.4). Such a mesh would have had far too many elements to be possible to run in a transient model.

Numerous studies have shown that the v2f model is good at impingement simulations [3][4][11] and that they generally are better than other RANS model for this. An UDF from Hesch, Sanz and Klanatsky [7] [8] was in FLUENT but it was notoriously hard to converge. To come around this the very similar $\zeta - f$ model was also tested but with disappointing results.

5.3 Pipestress

The resulting forces on the coolant pipe was used as input in a already existing model of the piping system. This simulation was performed by a consultant at FS Dynamics.

,

Chapter 6

Results and discussion

6.1 Pressure build up

The resulting pressure build up from breakage of one of the main circulation pipes can be seen in figure 6.1. It can be seen that there will be an initial pressure wave pushing down in drywell which reflects at the bottom. After a short relaxation of this wave the pressure rises almost linearly.

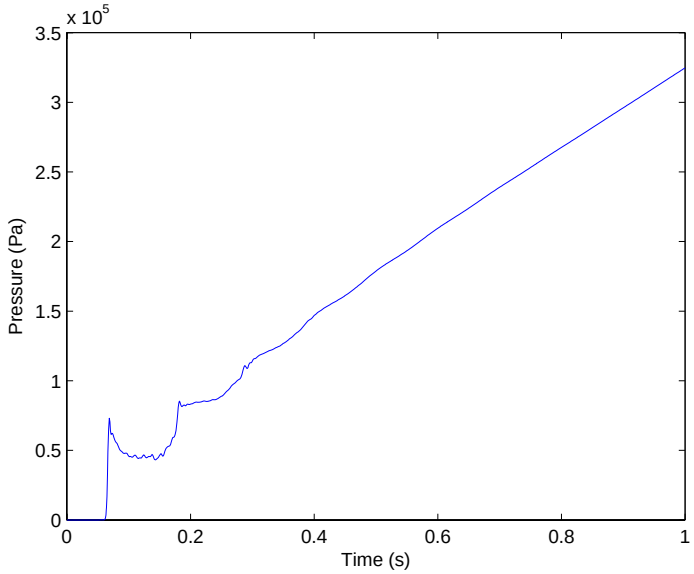

Figure 6.1: *The calculated pressure at the bottom of drywell during one second after a rupture on one of the main circulation pipes.*

These results are used as input in the FLUENT simulations but to account for the loss of pressure, when all the water has been blown out, the pressure

was held constant after this would have happened.

The choice of a one phase model with a lowered pressure after the blow-off of the jet can of course be discussed. After the water is blown out, steam enters the water pool forming a bubble interface against the water. This spreads out the static pressure over a larger area and doesn't focus it on just a column of water under the blowdown pipe. This makes it very probable that pressure on top of the jet would be drastically lowered. Steam gives a smaller contribution to momentum transfer since it is so much lighter than water. This is why it was argued to be conservative to use a continuous water jet but with a slightly lowered and constant pressure after the blow-off of the water jet.

6.2 Blown out jet

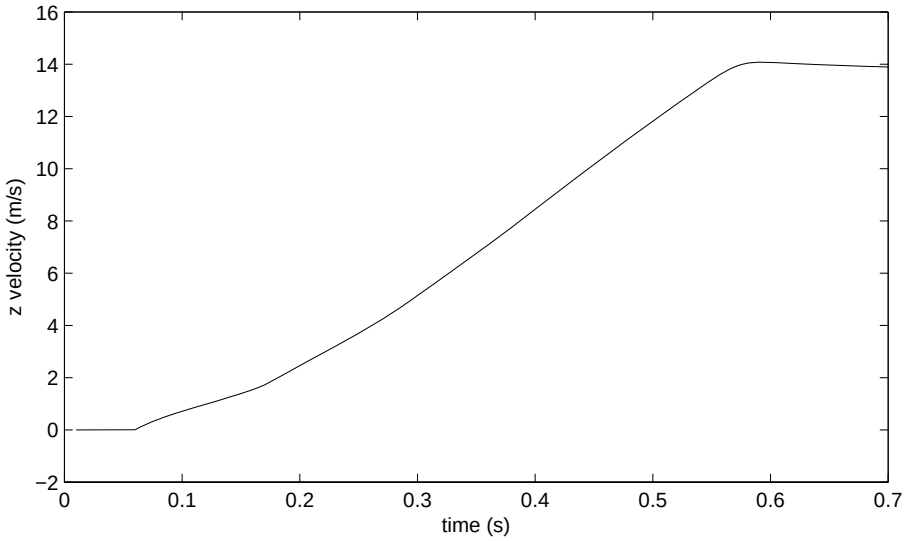

Figure 6.2: *The downward velocity at the inlet from the blowdown pipe into the water pool. With this the initial pile of water is blown out after 0.57s.*

Figure 6.2 shows the speed of the water passing the inlet at the end of the blowdown pipe. When integrated this gives that the originally 3m water cylinder will have been completely blown out 0.57 seconds after the breakage. Figure 6.3 shows the course of the jet when it hits the horisontal pipe from the time that the jet is completely blown out until when the main pressure

peak hits the pipe. The first large forces starts to appear after 0.8s and the head of the jet has passed soon after 1.0s.

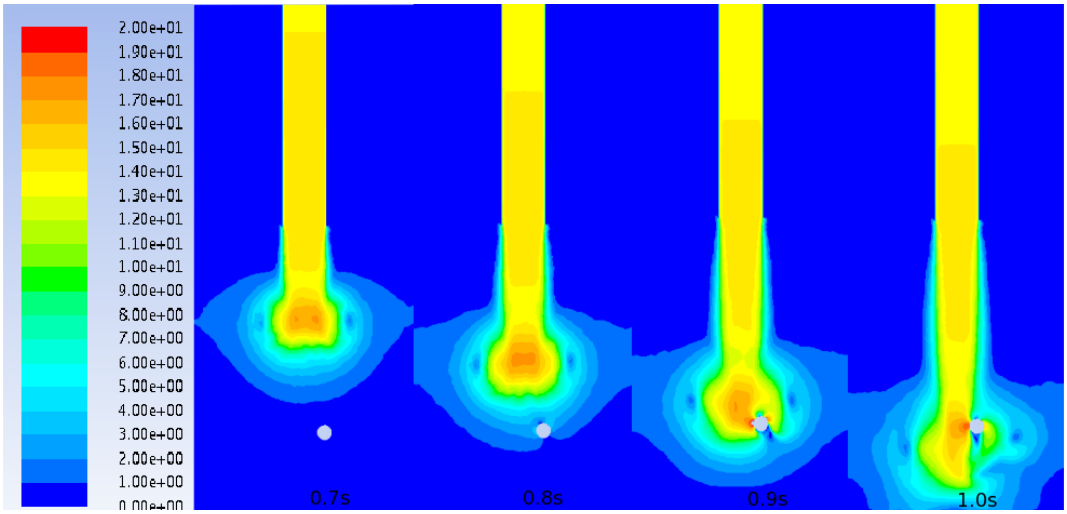

Figure 6.3: *Velocity contours for four different times during the simulation. This shows the course of the jet movements down to the pipe. The forces on the pipe starts at about 0.8s and reach their maximum around 1.0s*

6.3 Forces on the pipe

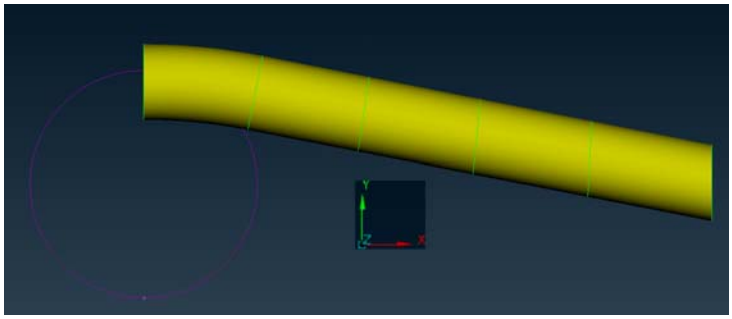

Figure 6.4: *The coolant pipe divided into five sections where the forces were calculated. The x-axis is along the pipe, the y-axis is upwards in the figure, away from the jet, and the z-axis is straight down. The purple line shows the diameter of the blowdown pipe.*

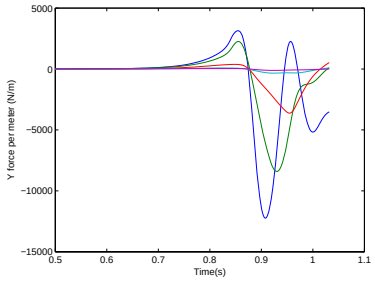

(a) Force in y-direction-original pipe

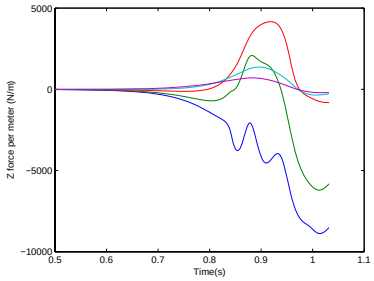

(b) Force in z-direction-original pipe

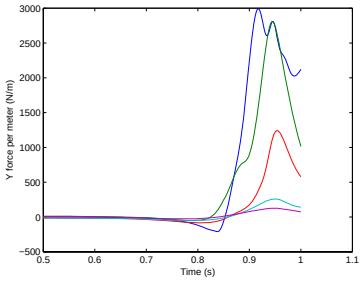

(c) Force in y-direction-centered pipe

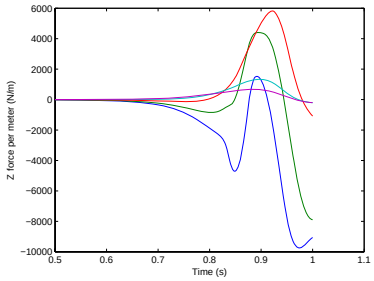

(d) Force in z-direction-centered pipe

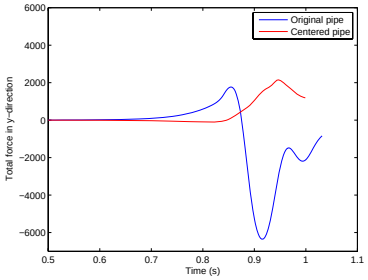

(e) Total force in y-direction for both pipes

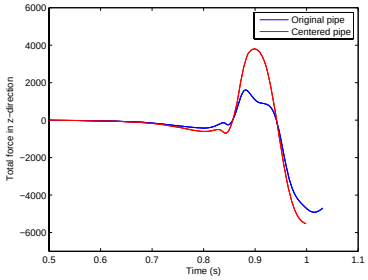

(f) Total force in z-direction for both pipes

Figure 6.5: *The forces on the pipe at the five sections where they are calculated. The blue line which also shows the greatest force is the section that lies fully within the jet. The two top figures show the forces on the original placing of the pipe and the two middle show the forces on a pipe centered under the jet. The last two show the total force on the pipe adding together all the sections.*

Figure 6.5 shows the downward and sideward force per meter acting on the pipe when hit by the water jet. These forces are calculated from the

static pressure on five sections of the pipe, each 30cm long which can be seen in figure 6.4. This data is used as input for the PipeStress model.

Starting with the discussion about the original placing of the horisontal pipe a few interesting things can be seen. There exists some oscillations in the forces. A lot of this can be explained by looking at figure 6.6. This shows the static pressure close to the pipe after 0.8s, i.e. just before impact. In front of the main jet there is a large pressure being built up as the dynamic pressure is transformed to static pressure against the pipe and the still water. The effect from this is seen in figure 6.5 as a positive force in the y-direction, i.e. away from the jet, as this spike presses from the inside of the pipe. In the z-direction it is visible as a slowly increasing force downwards.

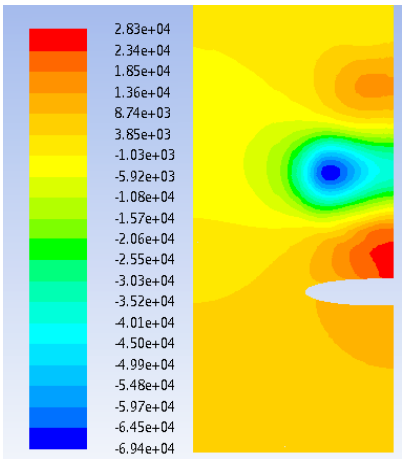

Figure 6.6: *The static pressure at 0.8s, i.e. right before impact, in the x-z plane cut in the middle of the pipe. The pipe doesn't lie straight in the plane, which is why not all of it is seen. The figure shows three distinct pressure areas. Positive pressure in front of the jet, a negative pressure wake in the shear layer and a secondary pressure peak.*

The second peak to reach the pipe is the circular pressure wake seen on the side of the jet. This is created from the large initial turbulence production when the jet first enters the pool and is transported downwards and amplified by additional turbulence production in the shear layer of the jet. When this reaches the top of the pipe, those parts of the pipe outside of the jet, are being pulled upwards and also the part under jet is slightly affected by this. In the y-direction these are not large enough to have a large effect however. It reaches the pipe at the same time as the main part of the jet reaches it, which greatly accelerates the water on the sides of the pipe. Especially on the inside of the pipe this gives high velocities and thus a low stagnation

pressure. This effect overshadows that of the wake and the pipe experiences a strong inward pull towards the center of the jet.

Thirdly a second wave within the jet reach the pipe and with this the same effects as from the first spike can be seen in both directions. When this has blown over, the pipe is again pulled inwards but the downward force from the continuous jet remains. Simulations after this are really unnecessary since all the water would now have passed the pipe if steam had been blown in the blowdown pipe instead of water.

The large inward horizontal force can also be explained when looking at figure 6.7. This shows pathlines for the jet calculated by FLUENT. The jet is deflected more to the right side, away from the jet. This sideways acceleration of the fluid requires a reaction force which comes from the pipe. This acceleration is why there is such a large inward force on the pipe.

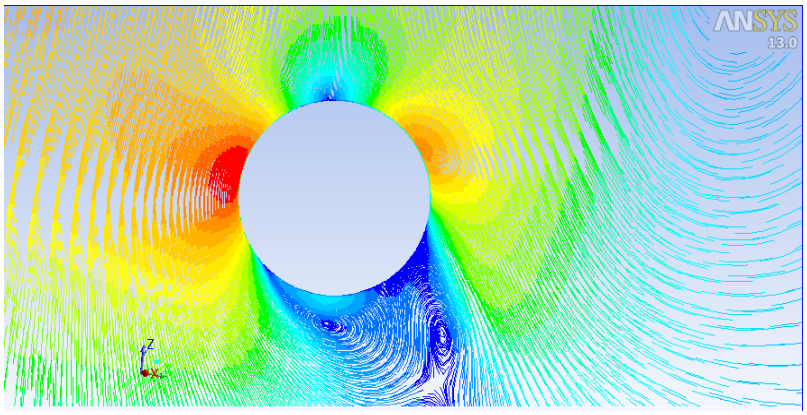

Figure 6.7: *Pathlines around the horisontal pipe for the jet calculated by FLUENT colored by velocity magnitude.*

The forces look a bit different when looking at the centered pipe. Since there is no asymmetric distribution of the velocities around the pipe, there aren't any large forces in the y-direction. The pipe is slightly bent however so when the low pressure wake hits the pipe it is slightly pulled outwards, away from the jet. These forces are a lot smaller than what can be seen for the original pipe.

In the z direction the forces are larger than the on the originally placed pipe. This can mainly be seen on the second part of the pipe. A larger part of this is exposed to the jet which of course gives larger forces.

An interesting result is seen in figure 6.8. It shows the resultant force $F_{\text{res}} = \sqrt{F_y^2 + F_z^2}$ for the two most inner parts of the pipe, for the two different placements of the pipe. The real placement of the pipe, i.e. asymmetrically under the jet, experience a higher total force than the one centered

under the jet even at the part secondmost closest to the jet center. So even though more of the pipe is exposed to the jet, the total force is mostly larger on the original pipe.

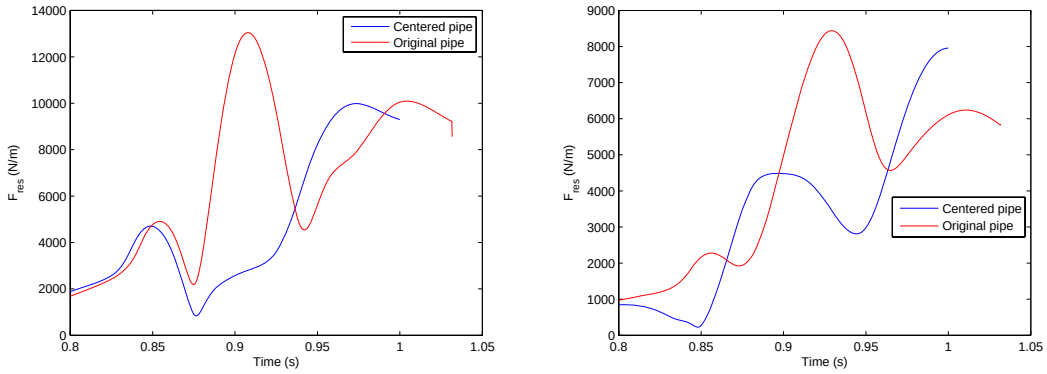

Figure 6.8: *The resultant force* $F_{res} = \sqrt{F_y^2 + F_z^2}$ *for the two placements of the pipes. The left figure shows the force on the part closest to the center of the jet and the right shows the forces on the second closest part.*

6.4 Jet profile around the pipe

The jet behaves a bit differently depending on the placement of the pipe. Figure 6.9 shows the velocities around the pipe. The pipe centered under the jet shows a very streamlined behaviour where the water returns under the pipe and the y-velocity thus is opposite under the pipe compared to above it. The momentum of the jet directly over the pipe is transferred to the sides of the pipe where the water is greatly accelerated. 100mm under the pipe the downward velocity profile is almost regained again except that the center is still slightly slower. Since so much of the momentum is retained the downward force on the pipe is not very large in comparison to the impingement against a flat surface.

The asymmetrical placed pipe shows slightly different velocity profiles around the pipe. The downward acceleration next to pipe isn't as pronounced and the y-velocity doesn't return as close to the pipe underneath it. Instead the water directly underneath the pipe shows a more turbulent behaviour with higher vorticity. This could be because the original pipe is hit by the shear layer of the jet where turbulence is high already before impingement. The downward momentum is fairly well regained 100mm under the pipe but

there is a clear positive net momentum in the y-direction which means that the pipe experiences a net force in the negative y-direction.

The asymmetric distribution of the velocities is also very clear in this figure. The downward velocity on the left, inner side is quite a lot larger than that of the outer side, giving the large differences in pressures which is responsible for the large sideward force. The same effect as seen with the pathlines, that the sideward acceleration of the water at the sides is greater can also be seen here.

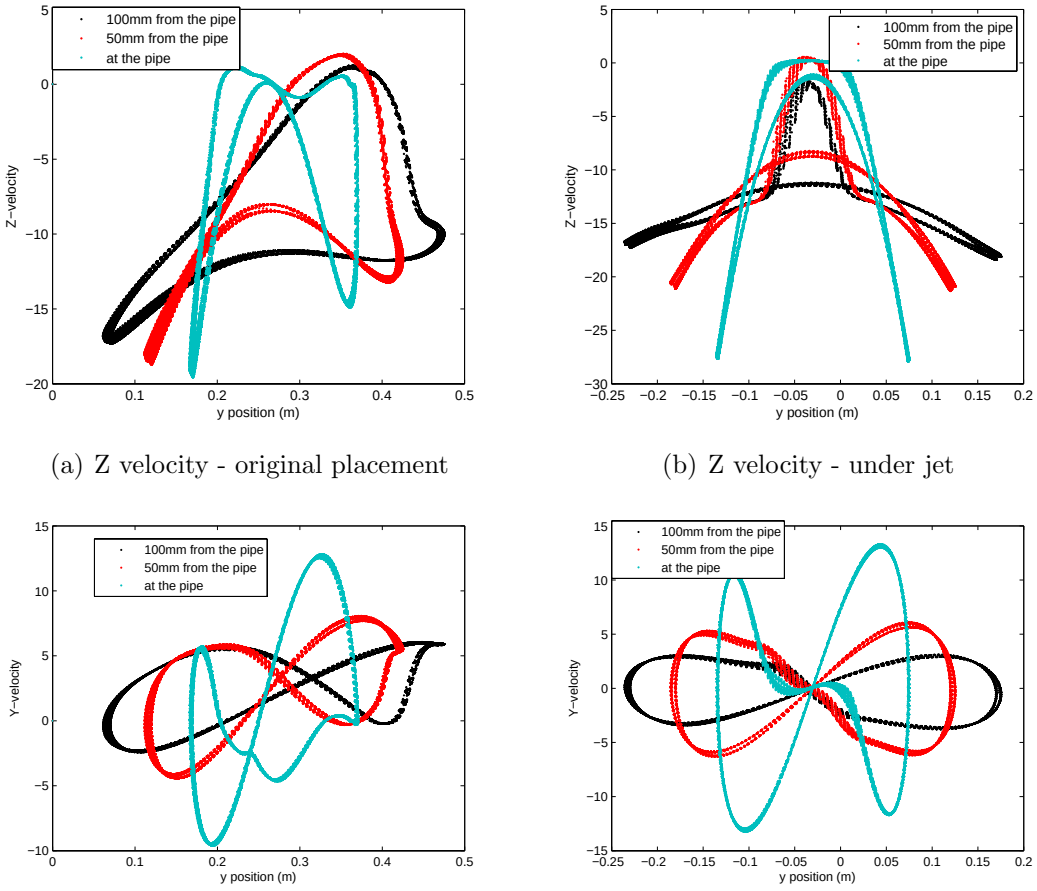

(a) Z velocity - original placement

(b) Z velocity - under jet

(c) Y velocity - original placement

(d) Y velocity - under jet

Figure 6.9: *Velocity profiles around the pipe at three different distances from the pipe, 0.5, 50 and 100mm at timestep 0.9s. To the left is the original placement of the coolant pipe, i.e. somewhat asymmetrically offset from the blowdown pipe and to the right the coolant pipe is placed straight under the jet.*

6.5 Choice of model

The choice of model is an important factor for the results. It would probably have been preferable to use a more sophisticated model since they are better at predicting correct turbulence for impinging jets. The main advantage of the $k-\epsilon$ model is its robustness which was the main problem when testing the v2f model. It is a known problem with the model that the equation for f often diverges and this was not overcome in these simulation. The simulation set up is problematic from a convergence point of view, with very high Reynolds number and impingement of a partially developed jet. Robustness was therefore an important feature in the choice of model.

LES needs a fine mesh to generate confident results. Again the problem with high Reynolds numbers combined with a large geometry gave length scales far too small for a transient LES simulation to be feasible. The problems with the convergence of the v2f model might also be referred back to the mesh size. Since the problematic part of the model is the f equation, which is the counterpart to the wall model for $k-\epsilon$, it is probable that it would be necessary to further refine the mesh close to the wall. The convergence problems occurred early in the simulation when velocities were still low so it is probable that a large refinement would have been necessary. It was not possible to increase the number of elements in the model that much since computational running times were already long. The only possible model to use was therefore the realisable $k-\epsilon$ model.

One problem with $k-\epsilon$ is that it overpredicts the production of k in the shear layer of the jet. This overprediction and subsequently also ϵ leads to a loss of energy in the shear layer and might be the reason for such a large negative pressure wake. The increased production of k also gives problems with the turbulent viscosity. Too high viscosity is unphysical and creates numerical problems. Most of the problems with the the turbulent viscosity emerge underneath the pipe where turbulence is high.

The unexpected result with the upward lift of parts of the pipe during a short time is not completely impossible but it seems a bit improbable that the net force on the pipe is upwards even during a very short time. This might have to do with a overprediction of the low pressure on beside the jet and might be further worsened by the numerical problems under the pipe.

6.6 Timescales

The timescale had an important role for the convergence of the solution. The courant number $C = \frac{v\Delta t}{\Delta x}$ is a nondimensional number used to relate the timestep size to the velocity and grid size. For an explicit solver the courant number is an absolute criteria for convergence of the solution but since an implicit solver has been used in this thesis, the courant number is more of a guideline. During the simulations a timestep size of 1ms was used giving a courant number of about 1 before the jet reached the pipe. The increased velocities around the pipe and the much finer mesh there required smaller timestep. The timestep was reduced to 0.25ms after 0.8s, just before impact. This allowed a converged solution with a courant number between 1 and 2 close to the pipe. To test the robustness of the solution it was also tested to reduce the timestep to 0.1ms, which gave an almost identical solution. This shows that the solution is independent of the timestep size at these scales.

6.7 Effects on the pipe

The forces on the pipe from the jet yields a utilisation of 95.3% when compared against the industrial standard ASME class 3 [5]. This shows that the reduction in conservatism, on the jets as made in this thesis, is possible.

6.8 Conclusions

The placement of the pipe clearly has a large effect on the forces from the jet. The original placement of the pipe gives a large sideward force that gives a higher total force than the pipe placed in the center of the jet.

The simulations shows that the forces are small enough for the coolant pipes not to break during a full scale LOCA. Since this is emergency pressure suppression system, the pipe only needs to hold for one jet and won't be exposed to these forces in normal usage of the reactor.

Impingement against a cylindrical body is not as well studied as impingement against a flat surface. When a jet impinges against a flat surface, all of its momentum in the normal direction of the wall is transferred to the wall. This is different in the cylindrical case when the jet is deflected around the jet and thus keeps a lot of its momentum. It is therefore not as obvious to say what the downward force should be but it is clear that the shape and the velocity of the jet around the pipe is of importance for the downward force.

The complexity of the problem is even further increased by the fact that it not a steady jet that is of interest. The head of the jet adds a couple of

extra features that are not seen in a steady jet. These are such as the low pressure wake in the shear layer and the pressure fluctuations in the front of the jet.

This complexity of the problem makes it probable that the $k - \epsilon$ realisable model is a bit inexact but other models are either too computational demanding or lacked robustness.

Bibliography

[1] a Group of Experts of the NEA/CSNI. Pressure supression system containments. Report, Commitee on the safety of nuclear installations, OECD nuclear energy agency, Paris, France, 1986.

[2] A. Bakker. Lecture 9 - kolmogorov's theory. http://www.bakker.org, 2006.

[3] M. Behnia, S. Parneix, and P. Durbin. Accurate modeling of impinging jet heat transfer. Technical report, Center for Turbulence Research, 1997.

[4] M. Bovo, S. Eternad, and L. Davidson. On the numerical modeling of impinging jet heat transfer. In *Int. Symp. on Convective Heat and Mass Transfer in Sustainable Energy*, Tunisia, 2009.

[5] ASME code. Asme code, section iii, division 1, nc-3600 2004 , addenda 06.

[6] L. Davidson. Fluid mechanincs, turbulent flow and sturbulence modeling. Course material, 25 February, 2011.

[7] Ch. Heschl, W. Sanz, and P. Klanatsky. Implemenation and comparison of different turbulence models for three dimensional wall jets with fluent. In *CFD Forum*, Bad Nauheim, Germany, 2005.

[8] Ch. Heschl, W. Sanz, and P. Klanatsky. Udf routine for fluent (v2f). http://www.fh-pinkaeld.ac.at/fhplus/eum/pdf/v2f.c, 2005.

[9] Y. Kukita, K. Namatame, and M. Shiba. The loca air-injection loads in bwr mark ii pressure supression containment systems. *Nuclear Engineering and Design*, 77(117-129), 1984.

[10] J. Marcinkiewicz and A. Lindgren. Förstudie av strömningsinducerade laster p interndelar vid brott i huvudcrikulationskretsarna i bwr. Report, SKI, 2002.

[11] A. Benavides Moran. Prediction of the axisymmetric impinging jet with different $k - \epsilon$ turbulence models. M. sc. thesis, Department of Thermo and FLuid Dynamics, Chalmers University of Technology, 2004.

[12] R. Peyret. Handbook of computational fluid mechanics. Academic Press Limited, USA, 1996.

[13] S. Pope. Turbulent flows. Cambridge University Press, 2000.

[14] RELAP5. Relap5/mod3.3 code manual volume i. Information Systems Laboratories, INC, Rockville Maryland, 2003.

[15] RELAP5. Relap5/mod3.3 code manual volume iv. Information Systems Laboratories, INC, Rockville Maryland, 2003.

[16] H. K. Versteeg and W. Malalasakera. Computational fluid dynamics, the finite volume method. Pearson education limied, England, 2007.

[17] D. Wilcox. Turbulence modeling for cfd. DCW Industries Inc, USA, 2007.

Appendix A: RELAP5 input file

```
0000001 0   *displays list of options
*+      8   *time step control due to void fraction change



****************************************
* Problem type and option (card 100)
****************************************
0000100 new transnt

****************************************
* Input check or run (card 101)
****************************************
0000101 run

****************************************
* Units selection (card 102)
****************************************
0000102 si si



************************************************************
* Noncondensable gas species (card 110)
************************************************************
0000110 air
0000115 1.0

0000201 29.7  1.00e-08 1.0e-02 15000 100     1000000 1000000
0000202 33.0 1.00e-08 5.0e-06 15000 100     1000000 1000000
0000203 35.0 1.00e-08 1.0e-02 15000 100     1000000 1000000


******************************************************
* Trips
******************************************************
20600000 expanded
*
20601070 time 0 ge null 0 22.0   n *Open after
20601080 time 0 lt null 0 28.0   n *Open valve
20601090 time 0 ge null 0 28.0   n *Close valve

20610010 107 and 108 n
```

```
*********************************************************
* Control variable numbers
*********************************************************
*
20500000 9999



****************************************
* Timedependent  001
****************************************
****************************************
*
*         Namn       Komponent
0010000    reaktor   tmdpvol
*
*         Area Length Volym A.vi In.vi Elevation Roughness Hyd.dia tlpvbfe
0010101    100.0  10.0   0   0.    0.    0.        0.      0.      0000000
*
*         ebt
0010200    103
*
*         Time      Pressure          Temp
0010201    0.0       70.0e+05   559.0 **TEMP



*********************************************************
* Time dependent junction 002
* from comp 001
* to comp 003
*********************************************************
0020000 unnamed tmdpjun
*       from      to        area   efvcahs
0020101 001010001 003010001  366.4e-3     000
* type
0020200 1
*       time   flowf flowg  velj
0020201  30.0    0.0   0.0   0.0
0020202  30.01    0.0  1880. 0.0
*********************************************************



*************************************************************************
* Primärutrymet, V = 5463 m3
* VL-220552
*************************************************************************
0030000   vl220552  pipe
*         number of volumes
0030001          50
*         x-coord volume flow areas  volume numbers
```

```
0030101    50.0                    5
0030102    90.0                    10
0030103    135.0                    15
0030104    185.17                    20
0030105    225.0                    25
0030106    250.0                    30
0030107    275.0                    35
0030108    300.0                    40
0030109    325.0                    45
0030110    350.0                   50
*        x-coord  volume lengths  volume number
0030301          0.5           50
*  Volume volume number volume number
*0030401  546.3                  10
*        vertical angles  volume number
0030601       -90.0              50
*        rough    hd  volume number
0030801   0.000045  0.0       50
*        fwd. loss  rev. loss  junction number
0030901      0.0        0.0         49
*        vol flags volume number
0031001        0         50
*        jun flags junc num
0031101      0       49
*        ebt    press   temp
0031201     4   1.0e+05 313.  1.0 0 0 50
*        ctrl word
0031300    1
*        flow66.9e-3f flowg velj junc num
0031301     0.0     0.0  0.0     49


**************************************************************************
* Initieringsvolym,
**************************************************************************
0040000 initvol   tmdpvol

*         Area Length Volym A.vi In.vi Elevation Roughness Hyd.dia tlpvbfe
0040101    100.0  10.0   0   0.    0.    0.        0.      0.      0000000
*
*         nebt
0040200    1104
*
*         Time      Pressure  Temp  steam    air.ratio
0040201    0.0       1.0e+05   313.0  1.0   0.01


**********************************************************
* valve 998 - Initventil0030101
* from comp 004
* to comp 001
**********************************************************
```

```
9980000 V2 valve

*       from      to          area   fwd.loss bwd.loss efvcahs
9980101 004010001 003250001   10.0     0.0       0.0    100
*       ctl flowf flowg velj
9980201 1     0.0  0.0   0.0
*
9980300 mtrvlv
*     opentrip closetrip rate   inipos table
9980301 1001      109     1000.0   0.0


. end
```

Appendix B:

```
#include "udf.h"
#include <math.h>

DEFINE_EXECUTE_AT_END(force_udf)
{§
#if !RP_HOST
      FILE *fp_y;
      FILE *fp_z;

      Domain *d;
      d = Get_Domain(1);     /* mixture domain if multiphase */
      Thread *ft, *ct;
      if(NULL == (ft = Lookup_Thread(d,4))) /* ID 4 is
bottenrÃ¶r*/
            Error("Something is wrong with ID 4!\n");

      if(!BOUNDARY_FACE_THREAD_P(ft))
            Message0("Warning ID 4 is not a boundary surface!
\n");

      #define nZones 5
      real force_x[nZones],Atot_x[nZones], Ftot_all[nZones];
      real force_y[nZones],Ftot_y[nZones],Atot_y
[nZones],Adiff_y[nZones];
      real force_z[nZones],Ftot_z[nZones],Atot_z
[nZones],Adiff_z[nZones];
      real buff[nZones], Antal[nZones];
      real coeff = 1/cos(10.0*3.14/90);
      real max_x = 1.5*coeff;
      /*printf("%g",coeff);*/
      int i;
      cell_t c0;
      face_t f;

      for(i=0;i<nZones;i++){
            force_x[i]=0;
            force_y[i]=0;
            force_z[i]=0;
            Ftot_y[i]=0,
            Atot_y[i]=0;
            Adiff_y[i]=0;
            Ftot_z[i]=0;
            Atot_z[i]=0;
            Adiff_z[i]=0;
            Antal[i]=0;
            Atot_x[i]=0;
            Ftot_all[i]=0;
      }
      real coord[ND_ND];
      real A[ND_ND];

      begin_f_loop(f,ft){
            c0 = F_C0(f,ft);
```

```
            ct = F_C0_THREAD(f,ft);
            if(NULL == ct)
                  Error("NULL pointer!\n");
            real vMag = cellVelocityMagnitude(c0,ct);
            real totP = F_P(f,ft)+0.5*C_R(c0,ct)*vMag*vMag;
            /*printf("%g \n", totP);*/
            F_CENTROID(coord,f,ft);
            F_AREA(A,f,ft);
            int pos;
            if(coord[0] < 0){
                  pos = 0;
            }else{
                  pos = nZones*coord[0]*coeff/max_x;
            }
            force_x[pos] += A[0]*totP;
            force_y[pos] += A[1]*totP;
            force_z[pos] += A[2]*totP;
            Adiff_y[pos] += A[1];
            Adiff_z[pos] += A[2];
            Antal[pos] +=1;

            /*if(totP > -100000000){*/
                  if(A[0]>0){
                        Atot_x[pos] += A[0];
                  }else{
                        Atot_x[pos] -= A[0];
                  }
                  if(A[1]>0){
                        Atot_y[pos] += A[1];
                        Ftot_y[pos] += A[1]*totP;
                  }else{
                        Atot_y[pos] -= A[1];
                        Ftot_y[pos] -= A[1]*totP;
                  }
                  if(A[2]>0){
                        Atot_z[pos] += A[2];
                        Ftot_z[pos] += A[2]*totP;
                  }else{
                        Atot_z[pos] -= A[2];
                        Ftot_z[pos] -= A[2]*totP;
                  }
                  Ftot_all[pos] += sqrt(A[0]*A[0]+A[1]*A[1]+A[2]
*A[2])*sqrt(totP*totP);
            /*}else{
            if(A[1]>0){
                        Atot_y[pos] += A[1];
                        Ftot_y[pos] -= A[1]*totP;
                  }else{
                        Atot_y[pos] -= A[1];
                        Ftot_y[pos] += A[1]*totP;
                  }
                  if(A[2]>0){
                        Atot_z[pos] += A[2];
                        Ftot_z[pos] -= A[2]*totP;
                  }else{
                        Atot_z[pos] -= A[2];
                        Ftot_z[pos] += A[2]*totP;
```

```
                }
        }*/
    }
    end_f_loop(f,ft)

    /* Average with the mean pressure around the part to
compensate for imperfect symmetry*/

    PRF_GRSUM(Atot_y,nZones,buff);
    PRF_GRSUM(Atot_z,nZones,buff);
    PRF_GRSUM(Ftot_all,nZones,buff);
    PRF_GRSUM(Adiff_y,nZones,buff);
    PRF_GRSUM(Adiff_z,nZones,buff);
    PRF_GRSUM(Ftot_y,nZones,buff);
    PRF_GRSUM(Ftot_z,nZones,buff);
    PRF_GRSUM(Antal,nZones,buff);
    PRF_GRSUM(force_x,nZones,buff);
    PRF_GRSUM(force_y,nZones,buff);
    PRF_GRSUM(force_z,nZones,buff);

    if(myid == 0){
        for(i=0;i<nZones;i++){
            printf("\n %g %g %g",force_y[i],force_z
[i],Ftot_all[i]);
            force_y[i] -= Ftot_y[i] * Adiff_y[i]/Atot_z
[i];
            force_z[i] -= Ftot_z[i] * Adiff_z[i]/Atot_z
[i];

        }
    }
    real time = CURRENT_TIME;

    if(myid == 0)
    {
        fp_y = fopen("fy.txt","a");
        fp_z = fopen("fz.txt","a");
        fprintf(fp_y,"%g ", time);
        fprintf(fp_z,"%g ", time);
        for(i=0;i<nZones;i++){
            fprintf(fp_y,"%g ", force_y[i]);
            fprintf(fp_z,"%g ", force_z[i]);
        }
        fprintf(fp_y,"\n ");
        fprintf(fp_z,"\n ");
        fclose(fp_y);
        fclose(fp_z);

        fflush(stdout);
    }
#endif
}
```